ORIGINAL ARTICLE

The reversal of drug resistance by two-dimensional titanium carbide Ti$_2$C (2D Ti2C) in non-small-cell lung cancer via the depletion of intracellular antioxidant reserves

Yue Zhu | Baiyan Sui | Xin Liu | Jiao Sun (ORCID)

Department of Dental Materials, Shanghai Biomaterials Research & Testing Center, Ninth People's Hospital, College of Stomatology, Shanghai Jiao Tong University School of Medicine, National Clinical Research Center of Stomatology, Shanghai Key Laboratory of Stomatology & Shanghai Research Institute of Stomatology, Shanghai, China

Correspondence
Jiao Sun, Department of Dental Materials, Shanghai Biomaterials Research & Testing Center, Ninth People's Hospital, College of Stomatology, Shanghai Jiao Tong University School of Medicine, National Clinical Research Center of Stomatology, Shanghai Key Laboratory of Stomatology & Shanghai Research Institute of Stomatology, No.427, Ju-men Road, Shanghai 200023, China.
Email: jiaosun59@shsmu.edu.cn

Abstract

Background: Chemoresistance is a major barrier limiting the therapeutic efficacy of late stage non-small cell lung cancer (NSCLC). In this study, we sought to use two-dimensional titanium carbide (2D Ti$_2$C) to reverse cisplatin resistance in NSCLC.

Methods: We first achieved favorable properties as a potential anti-tumor agent. We then compared cell viability and cisplatin uptake in chemoresistant NSCLC cells before and after the use of 2D Ti$_2$C. Afterwards, we explored the effects of 2D Ti$_2$C on intracellular antioxidant reserves, followed by evaluating the subsequent changes in the expression of core drug resistance genes. Finally, we confirmed the tumor inhibitory effect and bio-safety of 2D Ti$_2$C in a drug-resistant lung cancer model in nude mice.

Results: Due to the properties of thin layer, large specific surface area, and abundant reactive groups on the surface, 2D Ti$_2$C can deplete the antioxidant reserve systems such as the glutathione redox buffer system, γ-glutamylcysteine synthetase (γ-GCS), glutathione peroxidase (GPx), glutathione-S-transferase-Pi (GST-π), and metallothionein (MT), thereby increasing the intracellular accumulation of cisplatin and decreasing the expression of drug resistance genes.

Conclusions: 2D Ti$_2$C can reverse NSCLC chemoresistance both in vitro and in vivo, suggesting that it may potentially become a novel and effective means to treat chemoresistant NSCLC in the clinic.

KEYWORDS
2D Ti$_2$C, antioxidant reverses, drug resistance, NSCLC, reversal

INTRODUCTION

Chemotherapeutic drug resistance has been a critical challenge limiting the therapeutic efficacy of late-stage non-small-cell lung cancer (NSCLC) with a median survival of only 6 months.[1,2] Although the efficacy can be improved by increasing the dose of chemotherapeutic agents, using resistance site antagonists, or using genetic drugs, complications such as resistance to single drug, poor therapeutic efficacy, and indiscriminate killing of normal cells remain unresolved. Nanomaterials can often act against multiple specific targets in tumor cells due to their special physicochemical structure with limited toxic effects on normal cells,[3–6] gradually becoming a new tool for reversing drug resistance. Iron oxide nanoparticles have been found to have the effect of reversing cisplatin resistance by decreasing the expression of transmembrane transporter proteins and consequently increasing the intracellular concentration of cisplatin.[7–9] However, their effectiveness is still limited because abnormal activities of intracellular antioxidant reserve systems can either inactivate or excrete chemotherapeutic drugs, indicating that in order to improve the reversal of drug resistance in tumor cells, we must focus on improving intracellular drug metabolism, which is responsible for intracellular transport and excretion of chemotherapeutic drugs. Two-dimensional (2D) titanium carbide (Ti$_2$C) has the advantage

of ultra-high specific surface area among 2D materials, and its extremely thin nano-layer thickness enables it to have higher cell membrane penetration compared to conventional nanoparticles.[10] In addition, its large specific surface area and high numbers of reactive groups on the surface can be used as potential sites for interactions with proteins that can impact their structures and functions. However, it is still unknown whether these advantages can be exploited to deplete the abnormal antioxidant reserve system in drug-resistant cells. An in-depth investigation into this question will potentially maximize the antitumor effects of 2D Ti_2C and provide new insights on how to overcome drug resistance in NSCLC.

Chemotherapeutic drugs induce drug resistance in NSCLC by various mechanisms, among which increased expression of genes that contribute to the antioxidant reserve system is a central factor limiting the efficacy of chemotherapeutic drugs. This system is specifically responsible for the intracellular transport and excretion of chemotherapeutic drugs while directing the expression of other downstream drug resistance genes,[11–15] and the macromolecules of this system are characterized by possessing a large number of highly reactive thiol groups.[16] The unique physicochemical properties of 2D Ti_2C are expected to counteract the intracellular antioxidant reserve because of its lamellar structure and ultra-high specific surface area, which make it more accessible to intracellular proteins, while electron-absorbing reactive groups such as —F, —O, and —OH on the surface can interact with thiol groups to disrupt the structure and function of drug-binding proteins. In addition, it has been found that 2D Ti_2C has a significant oxidative stress effect on tumor cells after cell entry,[17] suggesting that it may induce enough reactive oxygen radicals to counter the antioxidant reserve. Ti_2C has also been reported to induce cell death in a variety of tumor cells while minimally affect normal cells.[18,19] These features make Ti_2C a highly promising agent for overcoming drug resistance in NSCLC.

In this study, we explored the feasibility of reversing chemoresistance in NSCLC by utilizing the properties of 2D Ti_2C including thin-layer, extra-large specific surface area, and abundant surface reactive groups on the surface. First, we obtained 2D Ti_2C and characterized its physical properties. Based on the fact that cisplatin is the first-line chemotherapeutic agent for the treatment of late stage NSCLC,[20,21] we then evaluated the overall cell viability and apoptotic state after treating a cisplatin-resistant NSCLC cell line with cisplatin in the presence or absence of 2D Ti_2C. We then compared the changes in cisplatin uptake by tumor cells before and after the use of 2D Ti_2C by measuring the intracellular platinum element content. The effect of 2D Ti_2C on the antioxidant reserve system was evaluated by analyzing oxidative stress levels, total glutathione (GSH/GSSG) level, the levels and redox buffer ratio between reduced glutathione (GSH) and oxidized glutathione (GSSG), the expression of glutamylcysteine synthetase (γ-GCS), changes in glutathione peroxidase (GSH-Px) content, the expression of glutathione-S-transferase-Pi (GST-π) and metallothionein (MT), and the expression of subsequent core drug resistance genes. Finally, we used an in vivo lung cancer resistance model in nude mice to confirm the inhibitory effect and mechnism of 2D Ti_2C on drug-resistant tumors and to verify the biosafety of its use in vivo. Taken together, our results suggest that 2D Ti_2C can potentially become a novel therapy for treating chemoresistant NSCLC.

MATERIALS AND METHODS

Chemicals and reagents

Ham's F12K medium, RPMI-1640 medium, and phosphate buffer solution (PBS) were purchased from HyClone Laboratories Inc. Trypsin–EDTA (0.25%), fetal bovine serum (FBS), and penicillin–streptomycin solution were purchased from Gibco Laboratories Inc. Cisplatin was purchased from Sigma-Aldrich Laboratories. The CCK-8 assay kit was purchased from the Dojindo Chemical Research Institute. The Annexin V-FITC/PI assay kit was purchased from BD Biosciences. RNeasy Mini SYBR Premix Ex Taq and the PrimeScript 1st strand cDNA Synthesis Kit were purchased from Takara Bio Inc. The reactive oxygen assay kit, GSH/GSSG assay kit, western blot lysis buffer, phenylmethylsulfonyl fluoride (PMSF), western blot transfer buffer, and nitrocellulose membranes were purchased from Shanghai Biotechnology Co Ltd. γ-GCS and GPx assay kits were purchased from Shanghai Xinle Biotechnology Co Ltd. Bicinchoninic acid protein assay was purchased from Pierce. Primary antibodies GST-π, MT, multidrug resistance-1 (MDR-1), lung resistance protein (LRP), and β-microtubulin (β-tubulin), as well as horseradish peroxidase-conjugated anti-rabbit or anti-mouse IgG secondary antibodies, were purchased from Abcam. Enhanced chemiluminescence (ECL) chemiluminescence reagents were purchased from Millipore. High concentration matrigel was purchased from Corning.

Preparation of 2D Ti_2C

Two-dimensional Ti_2C was manufactured and supplied by the Shandong Xiyan New Material Technology Cooperation. The preparation method is described by Liu et al.[22] Briefly, 0.67 g of lithium fluoride was slowly dissolved in 10 ml of hydrochloric acid at a concentration of 6 mmol/L by stirring for 5 min. One gram of Ti_2AlC was then slowly added over 10 min and the solution was stirred at room temperature for 24 h. The solution was then washed with deionized water and centrifuged at 3500 rpm for 5 min six to eight times until the pH of the solution was greater than 6. The precipitate was collected and dissolved in 100 ml of water and sonicated for 3 h under an argon-protected atmosphere. The solution was then centrifuged at 3500 rpm for 1 h and the supernatant was collected.

Characterization of 2D Ti_2C

The elemental composition of the parent phase Ti_2AlC and 2D Ti_2C nanostructures were analyzed by X-ray photoelectron

spectrometry (XPS, AXIS UltraDLD). The nanolayer thickness of the prepared 2D Ti_2C was observed and analyzed by high-resolution transmission electron microscopy (TEM) on a JEM-2100 microscope (JEOL) and ortho-inverted atomic force microscopy (AFM) on an NTEGRA microscope (NT-MDT). The hydrated particle size and zeta potential of 2D Ti_2C in different solutions were analyzed by the NanoBrook Omni Particle Size and Zeta Potential Analyzer (Brookhaven Instruments Corporation). The specific surface areas of the parent phase Ti_2AlC and 2D Ti_2C were determined by an Autosorb iQ3 automated surface area and pore size analyzer (Quantachrome).

A549/DDP cell culture

Human NSCLC A549 cells were purchased from the American Type Culture Collection (ATCC). The cisplatin-resistant strain A549/DDP cells were generated by Shanghai Fuheng Biology Ltd. Briefly, A549 cells were initially incubated with 0.05 µg/ml concentration of cisplatin in the incubator at logarithmic growth stage. Then the cisplatin-containing culture medium was discarded and the culture was continued with regular culture medium, while the surviving cells grew slowly. After entering the logarithmic growth phase, the cells were incubated again with a gradually increasing concentration of cisplatin. Medium changes and passages were repeated until the cells could grow and be passaged stably with a final concentration of 2.0 µg/ml while obvious drug resistance was observed. Then A549/DDP cells were cultured in F12K medium containing 1 µmol/L cisplatin at 37°C with 5% CO_2. Culture medium was supplemented with 10% (v/v) FBS (Gibco), 100 U/ml penicillin, and 100 µg/ml streptomycin. Cell passaging was performed every 2–3 days.

Cell viability assay

A549/DDP cells were inoculated in 96-well plates at a density of 1×10^4 cells/well and cultured for 24 h in their respective medium. The medium was then replaced with serial dilutions of fresh medium containing Ti_2C (50–200 µg/ml), cisplatin (10 µmol/L), or cisplatin (10 µmol/L) + Ti_2C (100 µg/ml). Cell viability was measured at 24 h with a CCK-8 assay kit.

Intracellular localization of 2D Ti_2C

To observe the localization of 2D Ti_2C in cells, A549/DDP cells were exposed to Ti_2C (100 µg/ml) or cisplatin (10 µmol/L) + Ti_2C (100 µg/ml) for 24 h. The cells were then washed three times with cold PBS and fixed in 2.5% glutaraldehyde at 37°C for 24 h. The cells were collected with a spatula, pelleted by centrifugation, dehydrated, and embedded in ethoxylated resin. Embedded cells were then sectioned and visualized by TEM in parallel with energy dispersive X-ray spectroscopy (EDS) elemental composition scans (JEM-2100, JEOL) to assess the subcellular distribution and basic composition of 2D Ti_2C and cisplatin in A549/DDP cells.

Intracellular cisplatin aggregation

A549/DDP cells were inoculated in 100 mm culture dishes at a density of 5×10^5 cells per well and cultivated for 24 h. The cells were exposed to regular culture medium with no other supplements, or medium containing cisplatin (10 µmol/L), Ti_2C (100 µg/ml), or cisplatin (10 µmol/L) + Ti_2C (100 µg/ml) for 24 h. Cells were washed three times with PBS and harvested. Cell pellets were successively dissolved in 30% hydrogen peroxide and 33% concentrated nitric acid, and elemental measurements were performed by inductively coupled plasma mass spectrometry (iCAP Q ICP-MS; Thermo Scientific).

Annexin V-FITC/PI apoptosis assay

Normal, apoptotic, and necrotic A549/DDP cells were identified using the Annexin V-FITC/PI assay kit. A549/DDP cells were inoculated in six-well plates at a density of 1×10^5 cells per well and cultured for 24 h. Then the cells were exposed to regular culture medium alone or medium containing cisplatin (10 µmol/L), Ti_2C (100 µg/ml), or cisplatin (10 µmol/L) + Ti_2C (100 µg/ml) for 24 h. The cells were washed three times with cold PBS and harvested. The cell pellets were resuspended in 500 µl binding buffer and incubated with 3 µl Annexin V-FITC for 25 min at 37°C, followed by another incubation with 2 µl PI for 5 min. A 500 µl dilution of the sample, which contained at least 10^4 cells, was analyzed by flow cytometry and data were analyzed by InCyte software (Millipore).

Determination of γ-GCS and GPx level

The levels of γ-GCS and GPx after 24 h of exposure to F12K medium alone or medium containing cisplatin (10 µmol/L), Ti_2C (100 µg/ml), or cisplatin (10 µmol/L) + Ti_2C (100 µg/ml) were determined by enzyme-linked immunosorbent assay according to the manufacturer's instructions.

Real-time polymerase chain reaction assay

A549/DDP cells were seeded into six-well plates at a density of 1.2×10^5 cells per well for 24 h. After treatment with the same method as in the apoptosis assay section, total RNA was extracted using an RNeasy Mini Kit according to the manufacturer's protocol, and RNA concentration was measured with NanoDrop. Total RNA (1 µg) was reverse transcribed to cDNA using a PrimeScript First Strand cDNA Synthesis Kit in a total volume of 10 µl. Real-time polymerase chain reaction (RT-PCR) was performed in a Roche Sequence Detection System (LightCycler 96) with an RT-PCR kit (SYBR Premix EX Taq). Primer sequences are shown in Table 1. For PCR, SYBR Green (10 µl) was added to the primers and cDNA (1 µl) in a total volume of 20 µl. β-microtubulin was used as an endogenous control. All samples were analyzed in triplicate. Relative expression levels

were calculated with the $2^{-\Delta\Delta Ct}$ method and normalized to β-microtubulin Ct values.

Western blot assay

A549/DDP cells were addressed in the same way as in the apoptosis assay section, washed three times with PBS, collected with a cell scraper, and lysed in cold western blot lysis buffer containing 1% PMSF for at least 30 min. The lysates were centrifuged at 12000 rpm for 10 min at 4°C and the supernatants were collected for use. Protein concentration was determined by the bicinchoninic acid (BCA) assay. Equal amounts of lysate proteins (25 μg) were then separated on SDS-polyacrylamide gels (8–12% separation gels) and electrophoretically transferred to nitrocellulose membranes. After blocking in Quickblock solution (Beyotime) for 30 min at room temperature, the membranes were probed with antibodies against metallothionein (1:1000), MDR-1 (1:1000), LRP (1:2000), and β-microtubulin (1:5000) at 4°C overnight, washed with tris buffered saline with tween-20, and then incubated with horseradish peroxidase conjugated anti-rabbit IgG/anti-mouse IgG secondary antibody for 1 h at room temperature. Antibody-bound proteins were detected using ECL chemiluminescence reagents.

Intracellular ROS assay

Flow cytometry measurement of intracellular reactive oxygen species (ROS) production was performed using a dichlorodihydrofluorescein diacetate (DCFH-DA) fluorogenic probe. DCFH-DA stock solution was diluted 1000-fold in serum-free cell culture medium to obtain a 10 mM working solution. After treatment with the same method as in the apoptosis assay section, cells in six-well plates were washed three times with PBS and incubated in 1 ml of DCFH-DA working solution for 30 min at 37°C in the dark. Cells were then washed and resuspended in cold PBS, and intracellular ROS was analyzed by flow cytometry (Guava easyCyte; Millipore). Data were normalized to the mean fluorescence intensity (MFI) values of control cells.

GSH and GSSG content analysis

A549/DDP cells were inoculated in six-well plates at a rate of 1×10^6 cells/well. After treatment with the same method as in the apoptosis assay section, cells were washed three times with PBS. Cells were collected in centrifuge tubes after trypsinzation, and then mixed with three volumes of Protein Removal Reagent M solution. Cell lysis was achieved by three freeze–thaw cycles with liquid nitrogen and 37°C water. The lysates were centrifuged at 12 000 rpm for 15 min at 4°C and the collected supernatants were used for GSH and GSSG assays. The amounts of total (GSH + GSSG), reduced (GSH), and oxidized (GSSG) GSH were obtained using the GSH/GSSG assay kit according to the manufacturer's protocol.

Animal experiments and sample collection

The experimental protocol was approved by the Animal Care and Medical Ethics Committee of the Shanghai Ninth People's Hospital, affiliated with Shanghai Jiaotong University School of Medicine. Female thymus-free nude mice (BALB/c, 4 weeks old) were obtained from Shanghai Jiagan Biotechnology Co. Mice were placed in sterile cages under a laminar flow-through air hood in a local SPF laboratory animal facility with a 12-h light/dark cycle, constant temperature (25°C), and relative humidity (50%). All animals were allowed free access to normal mouse food and water. After 1 week of acclimation, a A549/DDP-resistant xenograft model was established by subcutaneously injecting each nude mouse with 0.2 ml of A549/DDP cell suspension mixed with high concentration matrigel (2×10^7 cells/ml) into its left axilla. Tumor size was measured every 3 days after inoculation, and its long diameter a and short diameter b were recorded. Tumor volume was calculated by the formula $V = a \times b^2/2$. After the subcutaneous graft tumors rose to an average of 70 mm³, the xenograft mice were randomly divided into four groups ($n = 6$), namely, saline (0.5 ml) group, cisplatin-only (10 μmol/L) group, Ti$_2$C-only (100 μg/ml) group, and cisplatin (10 μmol/L) plus a Ti$_2$C (100 μg/ml) group. The mice were injected every 3 days while tumor size was recorded and the behavioral status of the mice was observed. At day 21, the animals were sacrificed, tumor tissues were harvested, and tumor size was measured.

Tumor tissues and other normal tissues (heart, liver, spleen, lung, and kidney) were collected seperately. Tumor

TABLE 1 PCR primer design

Target gene	Forward primer sequence (5′–3′)	Reverse primer sequence (5′–3′)
Bcl-2	GATTGTGGCCTTCTTTGAG	CAAACTGAGCAGAGTCTTC
Caspase-3	TTGACCTCAGCGCTGAGTTG	CCTGTAGCCCACGTCGTAGC
GST-π	ACCTCCGCTGCAAATACATC	GGTTAGGACCTCATGGATCA
Metallothionein-1	ATGGACCCCAACTGCTC	CAGCCCTGGGCACACTTG
MDR-1	CCCATCATTGCAATAGCAGG	TGTTCAAACTTCTGCTCCTGA
MRP	TGAAGGACTTCGTGTCAGCC	GTCCATGATGGTGTTGAGCC
LRP	GTCTTCGGGCCTGAGCTGGTGTCG	CTTGGCCGTCTCTTGGGGGTCCTT
β-tubulin	TCTACCTCCCTCACTCAGCT	CCAGAGTCAGGGGTGTTCAT

tissues were collected and the following RT-PCR steps including total RNA extraction, cDNA reverse transcription and RT-PCR were the same as those in vitro cellular experiments. The remaining tissue samples from all the mice from all groups were collected and fixed in 10% formalin for histopathological evaluation.

Statistical methods

All data are expressed as mean with standard deviation. All analyses were performed in Statistical Package for Social Sciences version 20.0 (SPSS Inc). Differences were assessed using Student's t-test or ANOVA. $p < 0.05$ indicates a statistically significant difference.

RESULTS AND DISCUSSION

Chemoresistance has been a major barrier limiting the therapeutic efficacy of late-stage NSCLC, and one of the keys to overcome the resistance lies in effectively countering the abnormally high intracellular antioxidant reserve. One promising approach is to use nanomaterials such as 2D Ti_2C with small size and large specific surface area, which can promote the generation of excess ROS,[7,23,24] release ions that bind to functional groups of intracellular proteins or nucleic acid molecules,[25] and alter cell membrane adhesion and permeability.[26,27] In addition, 2D Ti_2C also contains reactive groups such as –OH and –O on its surface, which can interact with sulfhydryl groups on molecules or proteins of the cellular antioxidant reserve system to disrupt their structures and functions. Exploring the drug-resistance reversal function of 2D Ti_2C is of great significance to improve chemotherapy efficacy, improving the prognosis of NSCLC patients and limiting drug side effects. In this study, we showed through both in vitro and in vivo experiments that 2D Ti_2C nanosheets can promote the death of drug-resistant NSCLC cells by depleting the intracellular antioxidant reserve, which in turn increases the effective accumulation of cisplatin in cells and decreases the expression of drug resistance genes.

Fabrication of ultra-thin 2D Ti_2C with large specific surface area and enriched in surface active groups

To maximize the interaction between 2D Ti_2C and lung cancer cells, the key factor is to fabricate 2D materials with the thinnest layer possible and a large amount of —OH, —O, and —F on the surface, for which a traditional top-down direct etching and ultrasonic fragmentation method was adopted. The results of XPS experiments show that, compared with the parent phase Ti_2AlC (Figure 1(a),(b)), the prepared particles no longer contained aluminum (Figure 1 (e),(f)), which confirms that the acidic etching effect of HF

has completely removed the original parent phase, meanwhile a large number of reactive groups such as —OH, —O, and —F, have newly appeared on its surface (Figure 1(c),(d), (g),(h)). To further separate the stacked etched products, we used ultrasonic disintegration to obtain the final products at nanoscale. Surface area analysis also revealed that the specific surface area of the 2D Ti_2C layer was significantly enhanced compared to that of the Ti_2AlC parent phase before etching. Quantitatively, we found that the Brunauer-Emmett-Teller (BET) specific surface area value of 2D Ti_2C (333.963 m^2/g) is nearly 100 times higher than that of Ti_2AlC (3.871 m^2/g) (Figure 1(m)). The high specific surface area combined with the large number of reactive groups possessed by 2D Ti_2C may provide an important advantage for enhanced interaction with cellular macromolecules.

To evaluate the particle size and stability of 2D Ti_2C in solution, we assessed its hydrated particle size and zeta potential, and the results showed that the hydrated particle size increased slightly in neutral and acidic ionic buffers compared with the original solid state, both maintaining at approximately 250 nm (Figure 1(n)), while the absolute value of zeta potential increased significantly in acidic solutions compared with neutral solutions (Figure 1(o)), suggesting that 2D Ti_2C is more stable and less likely to accumulate in acidic solutions than neutral solutions, which is consistent with the previous study by Jastrzębska et al.[28] Tumor tissues are usually in a weak acidic environment, and nonaccumulation in weak acid is crucial to maintain the 2D Ti_2C thin-layer structure, while lower lamellae thickness is more favorable for the nanosheets to act directly through the cell membrane.[29] Furthermore, the relatively increased aggregation in a neutral environment also reduces the uptake of 2D Ti_2C by normal cells. Therefore, these data showed that our fabrication method can produce 2D Ti_2C nanosheets with desirable properties for potentially specific activity against tumor cells.

2D Ti_2C re-sensitizes A549/DDP cells to cisplatin

To assess the effects of 2D Ti_2C on the viability of cisplatin-resistant A549/DDP cells, we first evaluated cell growth after 24 h of treatment with the nanomaterial in the absence or presence of cisplatin. Interestingly, we noticed through a dose–response experiment that 2D Ti_2C alone significantly inhibited the growth of A549/DDP cells at concentrations of 100 and 200 μg/ml (Figure 2 (a)). We also observed, as expected, that 10 μM cisplatin failed to inhibit cell growth (93.62% $\pm$ 1.67%), whereas the same concentration had been shown to inhibit the growth of nonresistant cancer cells.[30–32] The combination treatment of 100 mg/L Ti_2C with 10 μM cisplatin further inhibited cell growth (45.70% $\pm$ 3.63%) by ∼20% compared with 100 mg/L Ti_2C alone (64.10% $\pm$ 4.53%) (Figure 2(a)), suggesting that cisplatin sensitivity was partially restored by 2D Ti_2C.
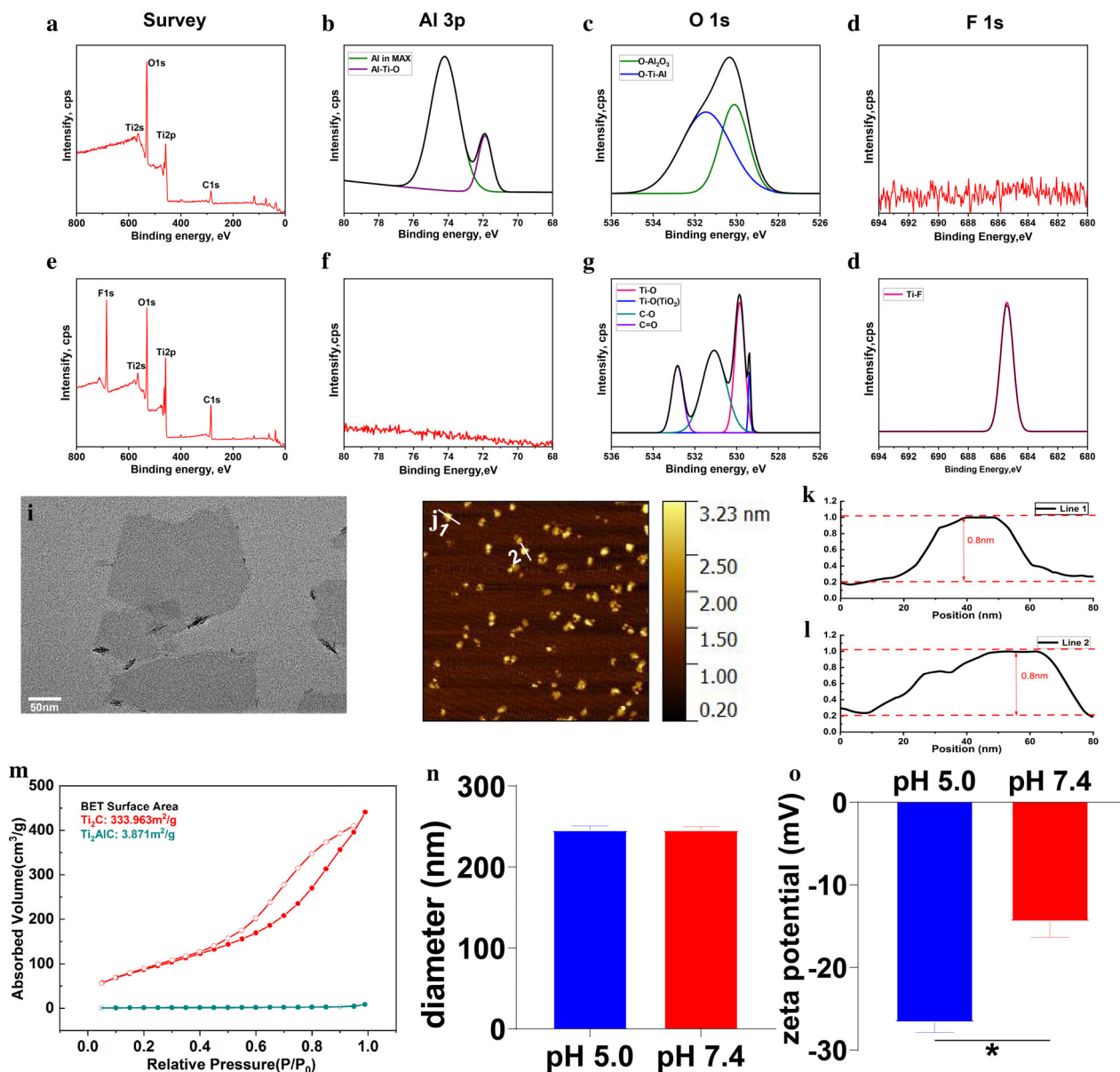
FIGURE 1 Characterization of 2D Ti$_2$C nanoparticles. High-resolution XPS spectra. Survey spectra of Ti$_2$AlC (a) and Ti$_2$C (e), Al3p, O1s, F1s spectra of Ti$_2$AlC (b–d) and Ti$_2$C (f–h). TEM image of Ti$_2$C (i). AFM image of Ti$_2$C (j) and its related analysis file (k, l). Adsorption/desorption isotherms of Ti$_2$C (m). Dynamic light scattering (n) and zeta potential of Ti$_2$C (o). *$p < 0.05$

Cisplatin is a first-line chemotherapeutic agent for the treatment of late-stage NSCLC, which initiates apoptosis-mediated killing by cross-linking with DNA in the nucleus and induces the intrinsic apoptosis pathway involving the formation of the apoptosome and caspase activation. To determine whether the growth inhibition we observed resulted from cell death, we evaluated the percentages of dying cells and the expression level of Bcl-2 and caspase-3 after treatment with 2D Ti$_2$C and/or cisplatin We found that 2D Ti$_2$C alone significantly increased the apoptotic/necrotic rate of A549/DDP cells (38.04% ± 1.57%) (Figure 2(b),(c),(e)), consistent with the results of the cell viability assay (Figure 2(a)). By comparison, cell death was further enhanced (67.41% ± 2.92%) after the combination treatment (Figure 2(b),(c),(f)), suggesting that cisplatin was able to activate apoptosis in the

presence of 2D Ti$_2$C. Induction of apoptosis by 2D Ti$_2$C with or without cisplatin was further validated by the down-regulation of Bcl-2 (Figure 2(g)), an inhibitor of apoptosis, and the upregulation of caspase-3 (Figure 2(h)), a central protease in the apoptotic process. Collectively, these data showed that 2D Ti$_2$C not only induces cell death but also re-sensitizes chemoresistant cells to cisplatin.

2D Ti$_2$C increases the intracellular accumulation of cisplatin

The sublocalization of drugs and nanoparticles in the cellular organelles can directly determine where and if they can exert their expected biological effects. For cisplatin, its
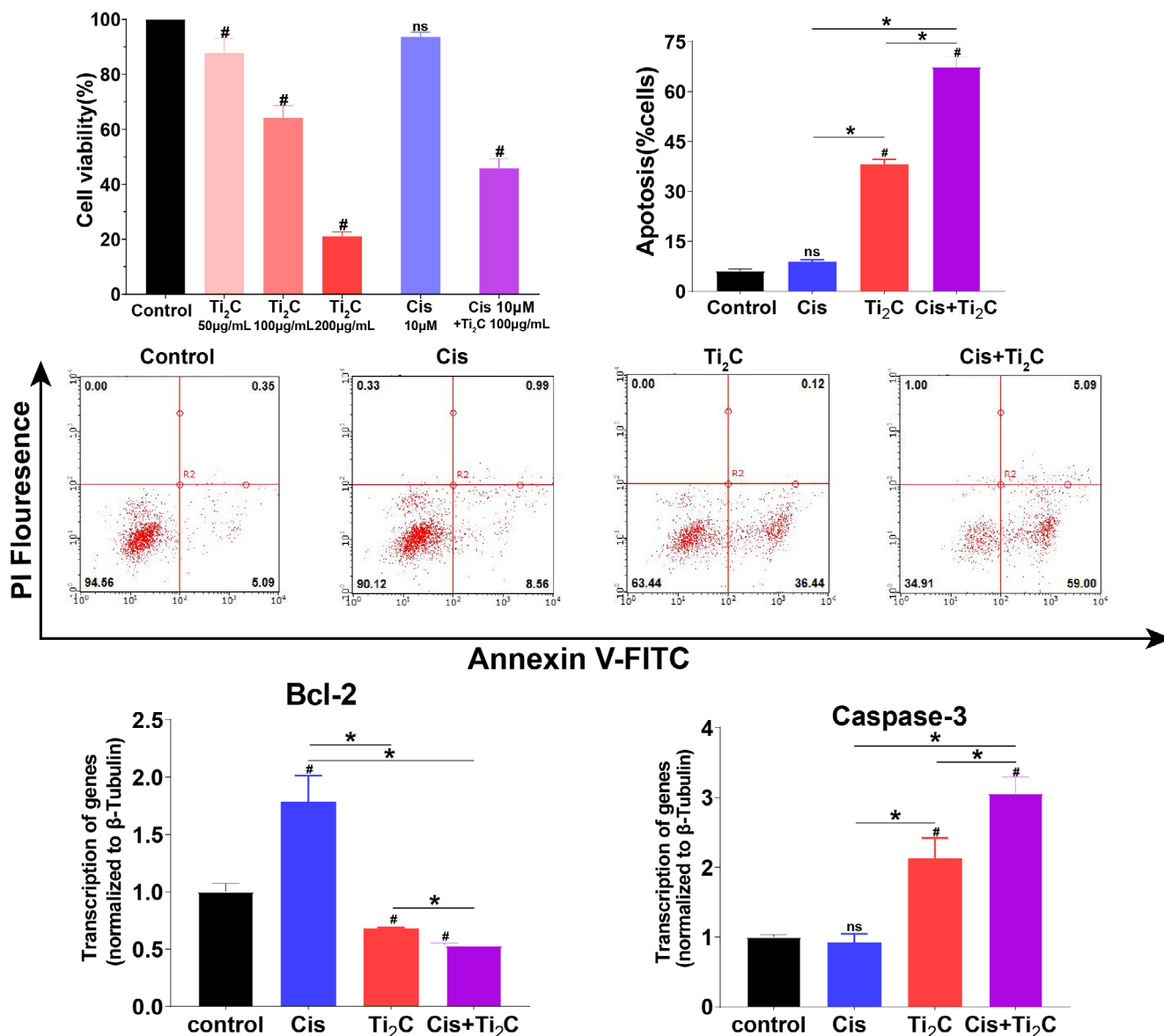
FIGURE 2 Cytotoxic and apoptotic effects of cisplatin and 2D Ti$_2$C on A549/DDP. Cell viability of A549/DDP cells after exposure to 2D Ti$_2$C, cisplatin, and cisplatin plus 2D Ti$_2$C (a); apoptotic ratios from Annexin V-FITC/PI double staining ($n = 3$) (b); dot plots of Annexin V-FITC/PI staining of A549/DDP cells that were untreated (c), treated with cisplatin (d), treated with 2D Ti$_2$C (e), or treated with cisplatin plus 2D Ti$_2$C (f), representatively; Bcl-2 mRNA expression in A549/DDP (g); Caspase-3 mRNA expression in A549/DDP (h). *$p < 0.05$. # indicates a significant difference with the control group. ns indicates not significant with the control group

successful accumulation inside the nucleus is one of the necessary conditions for it to exert its cytotoxic effects on the cells. Therefore, we evaluated the localization and concentration of cisplatin and 2D Ti$_2$C in A549/DDP cells by electron microscopy and ICP-MS. Cisplatin treatment alone did not result in its localization into the nuclei, and there was also very low cytoplasmic accumulation (Figure 3(a)–(c)), suggesting that one possible mechanism of resistance in these cells was by blocking cisplatin entry and/or accumulation in the nucleus or cytoplasm. A large number of nanoparticles was found to be clustered in the cytoplasm after treating A549/DDP cells with 2D Ti$_2$C (Figure 3(d), (e)), which suggests that 2D Ti$_2$C can be effectively taken up

by drug-resistant A549/DDP cells, and that any drug resistance proteins expressed by these cells cannot effectively excrete 2D Ti$_2$C. One reason for this might be that the ultrathin nature of 2D Ti$_2$C allows it to create nano-scale pores on the tumor cell membrane, thereby allowing it to penetrate into the cytoplasm. This mechanism has already been confirmed in other 2D nanosheet layers.[33] The effective retention of 2D Ti$_2$C in the cytoplasm is also an important prerequisite for its subsequent functions. In contrast, 2D Ti$_2$C is not found in the nucleus (Figure 3(d),(f)), probably because its lateral size is not yet sufficient to simultaneously break through the nuclear pores. When A549/DDP was co-treated with both cisplatin and 2D Ti$_2$C, 2D Ti$_2$C remained
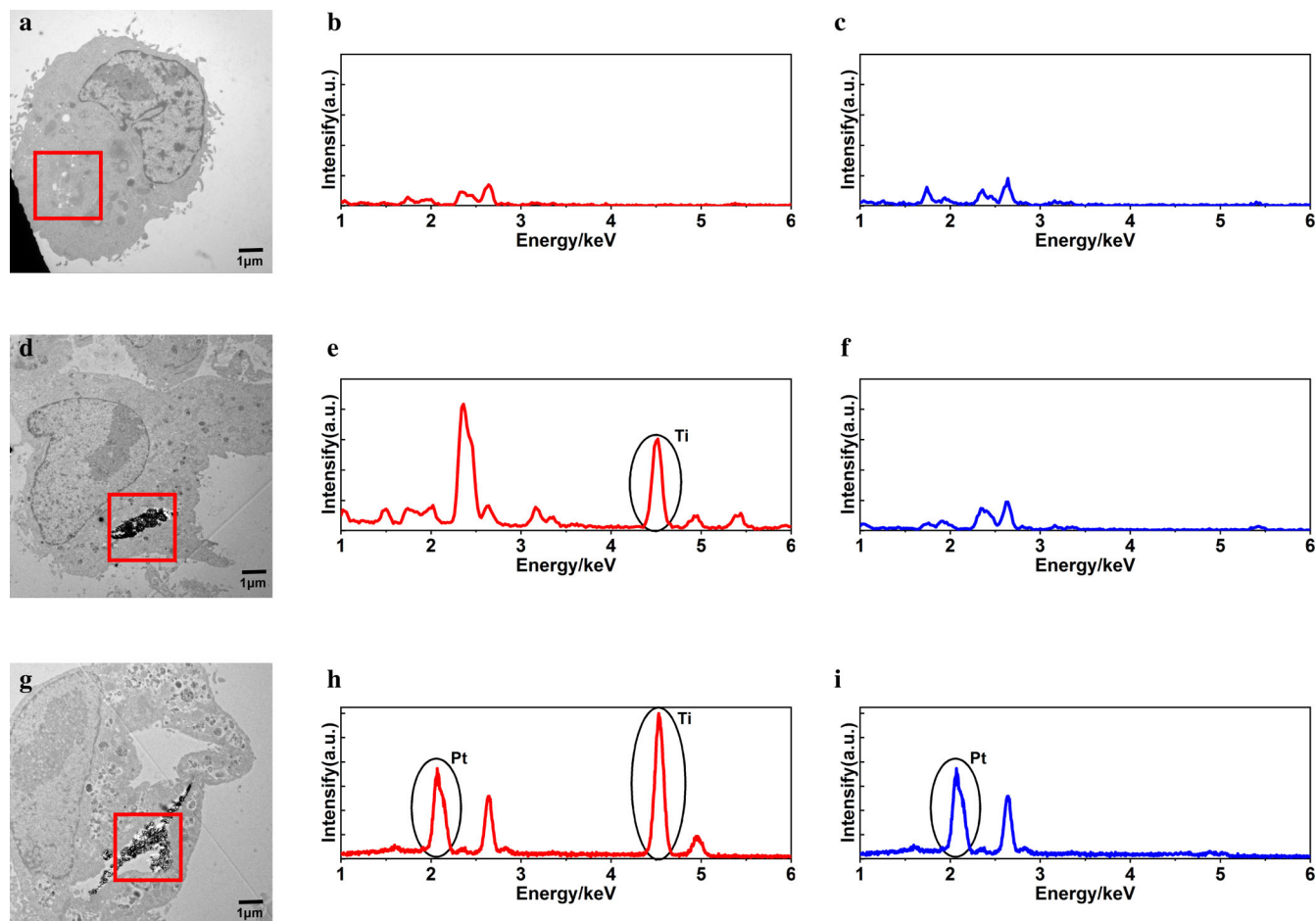
FIGURE 3 Uptake of cisplatin and 2D Ti$_2$C by A549/DDP. TEM micrographs of A549/DDP exposed to cisplatin (a), 2D Ti$_2$C alone (d), and cisplatin plus 2D Ti$_2$C (g). The corresponding chemical composition analyses of the particles using energy-dispersive X-ray spectroscopy (EDS) were shown in (b) and (c), (e) and (f), and (h) and (i) next to the micrographs. EDS analyses of the cytoplastic locations on the TEM images are indicated in red (b, e, h) and the nuclear regions in blue (c, f, i)

TABLE 2 Quantification of cellular uptake of cisplatin

Treatment	Control	Cis	Ti$_2$C	Cis + Ti$_2$C
Platinum concentration	0.10 ± 0.03	63.88 ± 5.48[a]	0.11 ± 0.02	505.15 ± 57.54[a,b]

Note: Quantification of cellular uptake of cisplatin after 24 h treatment with control, cisplatin, 2D Ti$_2$C, and cisplatin plus 2D Ti$_2$C, represented as Pt concentration (ppm) per 10^5 cells. Data represent the mean ± SEM ($n = 3$).
[a]Indicates statistical significance against control group.
[b]Indicates statistical significance against cisplatin group.

mainly in the cytoplasm while cisplatin was observed in both the cytoplasm and the nucleus (Figure 3(g)–(i)), suggesting that 2D Ti$_2$C was able to facilitate cisplatin entry into the nucleus. The effective concentration of cisplatin was elevated to about eight times that of cisplatin alone (Table 2). We speculated that the nano-scale pores created on the cell membrane by 2D Ti$_2$C allowed cisplatin to penetrate into the cytoplasm either alone or attached to 2D Ti$_2$C, thus bypassing the copper transporter protein uptake mechanism that cisplatin normally relies on.[34,35] This set of data collectively demonstrated that effective cytoplasmic accumulation of 2D Ti$_2$C itself and its facilitation of cisplatin influx

are important factors that contribute to the subsequent biological effects of both substances.

2D Ti$_2$C depleted intracellular antioxidant reserve

In the previous experiments we found that 2D Ti$_2$C has the effect of reversing cisplatin resistance in NSCLC. To investigate the underlying mechanism, we focused on the intracellular antioxidant system. An abnormal increase of antioxidant reserve is a central factor in cisplatin resistance.

In a chemoresistant NSCLC, even if a chemotherapeutic agent like cisplatin can successfully accumulate inside the cell, the antioxidant system can still sequester or even excrete the drug out of the cytoplasm,[36] and it can also signal the activation of DNA repair to counter any DNA damage from the chemotherapeutic agent.[37,38] Therefore, we looked into how 2D Ti₂C may impact the antioxidant system inside cisplatin-resistant tumor cells.

GSH is a central component of the antioxidant system and can protect cells in multiple ways. For example, GSH can conjugate with platinum drugs such as cisplatin and facilitate their efflux via multidrug resistant proteins (MRPs),[39] and it can also chelate copper and prevent it from participating in free radical generation.[40] The increase in total GSH and the increased proportion of GSH in tumor cells can enhance cellular resistance to cisplatin, and some studies have found that exogenous ROS can act directly on the GSH system of tumor cells.[41] In our study, we found that 2D Ti₂C promoted ROS production in A549/DDP cells, and ROS generation was further amplified after co-treatment with cisplatin (Figure 4(a)). Concurrently, we observed that the level of both total and reduced GSH (as implicated by the GSH:GSSG ratio) were significantly decreased after 2D Ti₂C treatment, and this effect was further enhanced after co-treatment with cisplatin (Figure 4(b),(c)). These results indicate that the redox system in the resistant cells is disrupted by 2D Ti₂C, and a reduction in both total GSH and GSH suggests that less GSH is available to neutralize ROS and xenobiotics.[42] Hence, depletion of GSH is a crucial step in 2D Ti₂C-mediated re-sensitization of cisplatin-resistant NSCLC cells.

However, GSH-mediated drug resistance is an integrated process, so it is possible that, after a disruption of the
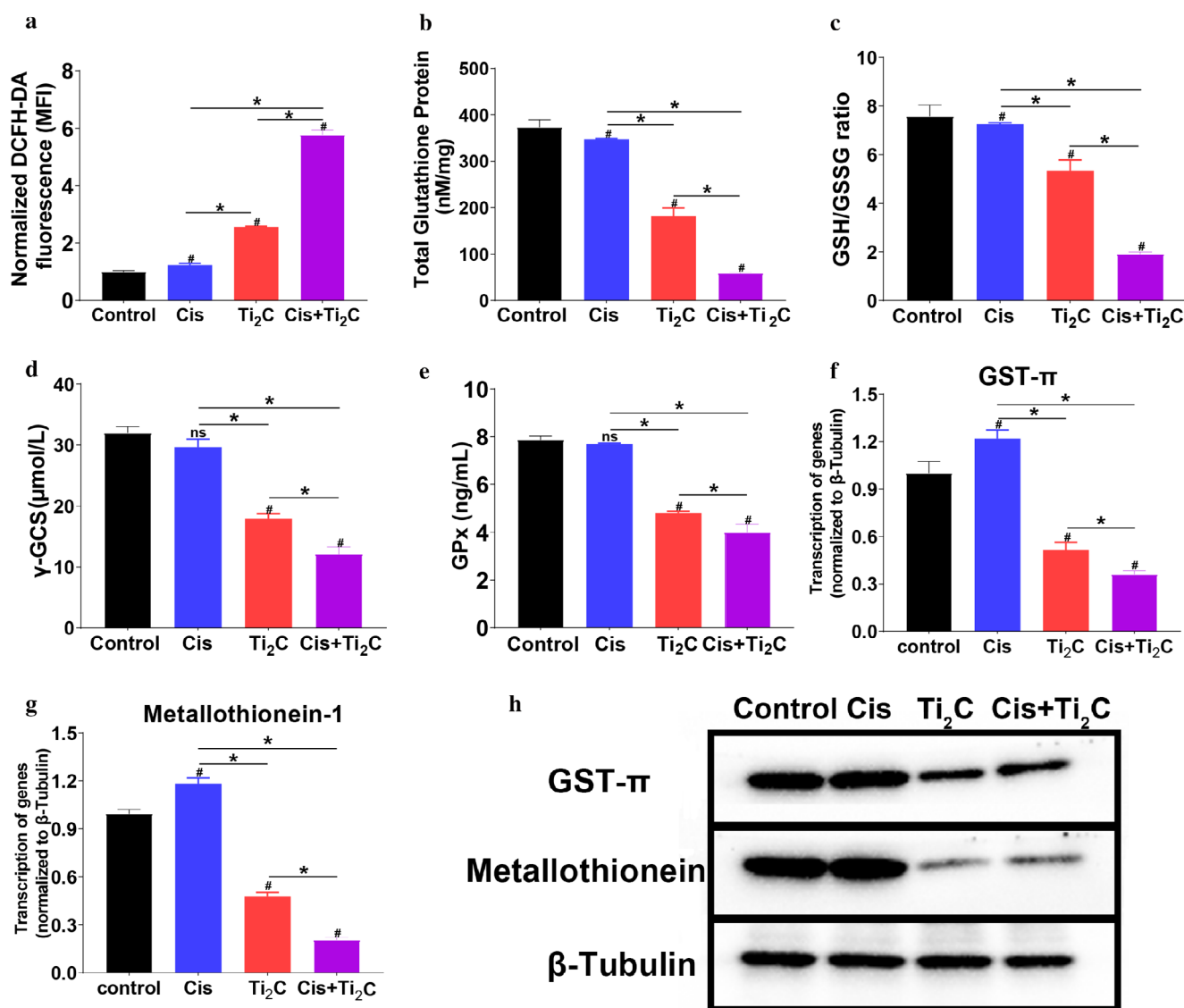

FIGURE 4 Depletion of intracellular antioxidant reserves in A549/DDP cells by 2D Ti₂C. Effects of 2D Ti₂C and cisplatin on reactive oxygen species (ROS) production (a), GSH levels (b), intracellular GSH/GSSG ratios (c), γ-GCS and glutathione peroxidase (GPx) levels (d, e), and GST-π and metallothionein mRNA expression (f, g) and protein expression (h). *$p < 0.05$. # indicates a significant difference with the control group. ns indicates not significant with the control group

GSH/GSSG redox buffer system, resistant cells may still restore it back to the previous level through some compensatory mechanisms. Therefore, to reverse drug resistance by depleting GSH to a greater extent, it would be necessary to target proteins involved in GSH production. γ- GCS is the rate-limiting enzyme for GSH biosynthesis in vivo, and its activity directly mediates the rise in intracellular levels of GSH. It has been found that NSCLC tissues showed higher uptake of GSH and increased γ-GCS enzyme activity compared to normal lung tissue.[43] Inhibition of γ-GCS can reduce intracellular GSH levels and thus reverse drug resistance, for which a specific inhibitor, buthionine sulfoximine (BSO), has been developed for γ-GCS and has been shown to be clinically effective.[44–48] Furthermore, even if GSH levels are temporarily reduced, tumor cells can mediate drug resistance by rapidly replenishing GSH through negative feedback regulation. We found that γ-GCS level was unchanged when A549/DDP cells were treated with cisplatin alone, and that it was decreased significantly when the cells were exposed to 2D Ti$_2$C with or without cisplatin (Figure 4(d)). It is possible that any depletion of GSH by cisplatin alone was immediately countered by the feedback activation of γ-GCS, while 2D Ti$_2$C appears to mitigate γ-GCS expression, which perhaps leads to the downregulation of GSH expression. GPx is a peroxidolytic enzyme highly expressed in drug-resistant tumor cells, and its active center contains selenocysteine, which catalyzes the reaction of GSH with H$_2$O$_2$ and prevents the latter from damaging cells by peroxidation.[49] Recent studies have

found that therapy-resistant breast, melanoma, and lung cancer cells exhibit enhanced sensitivity to GPx inhibitors.[50] Kui et al.[51] found that the high expression of GPx mRNA in patients is clinically important in indicating the prognosis of patients through analyzing the genetic data and survival information of 1926 NSCLC patients. In our study, the expression of GPx was significantly decreased after 2D Ti$_2$C treatment (Figure 4(e)), which is further indicative of disrupted GSH homeostasis.

In addition to the GSH/GSSG homeostatic system, the glutathione S-transferase (GST) family proteins and metallothioneins are also part of the antioxidant system. Among the four major isoforms of GST proteins, the overexpression of GST-π in tumors has been linked to therapeutic resistance.[52–54] GST-π can upregulate the survival signal of drug-resistant tumors by interacting with c-Jun N-terminal kinase (JNK), in addition to mediating its own binding to cisplatin and blocking the cisplatin entry pathway into the nucleus.[55] It has been well documented that GST-π is overexpressed in NSCLC and cisplatin is generally effective in tumors with low GST-π expression.[36,56,57] Gajra et al.[58] found that high expression of GST-π is an independent prognostic factor in resected stage I NSCLC. Metallothioneins are cysteine-rich proteins that scavenge metals and ROS through abundant thiol groups on the cysteine residues, thus playing a key role in the detoxification of heavy metal elements and counteracting mitochondrial stress.[59,60] They can also interact directly with chemotherapeutic drugs, and binding between
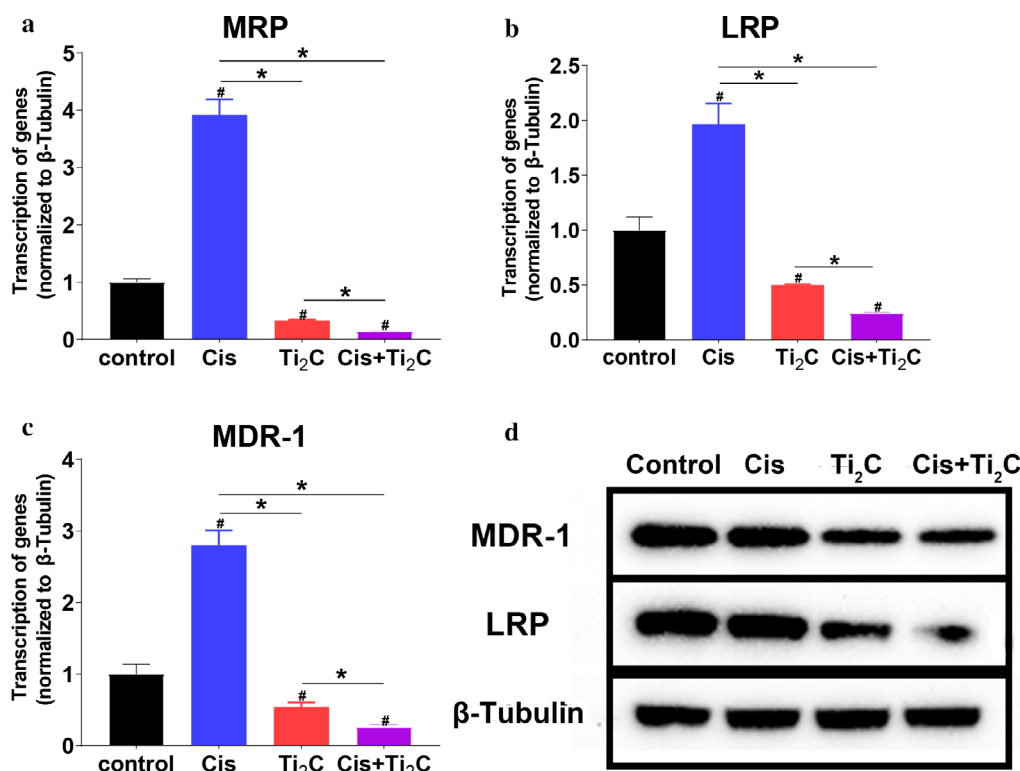

FIGURE 5 Expression of cisplatin resistance genes in A549/DDP cells: MRP mRNA expression (a), LRP mRNA expression (b), MDR-1 mRNA expression (c), and representative expression profile of proteins for MDR-1 and LRP (d). *$p < 0.05$. # indicates a significant difference with the control group

metallothioneins and the metal elements within drug molecules can disable their activity.[61,62] Borchert et al.[63] demonstrated that metallothionein knockout substantially reduced cisplatin resistance in malignant pleural mesothelioma. It has been found that the positive rate of metallothionein in tissue sections of NSCLC patients treated with cisplatin chemotherapy increases from 27% to 80%.[64] Based on these findings, we hypothesized that reducing the expression of GST-π and metallothionein would very likely reverse cisplatin resistance in NSCLC as well. In this study, we found that the expression of GST-π and metallothionein decreased significantly at both transcript and protein levels after treating A549/DDP cells with 2D Ti_2C, with or without cisplatin (Figure 4(f)–(h)). At the transcript level, the combination treatment downregulated both genes even further in comparison with 2D Ti_2C alone (Figure 4(f),(g)). These
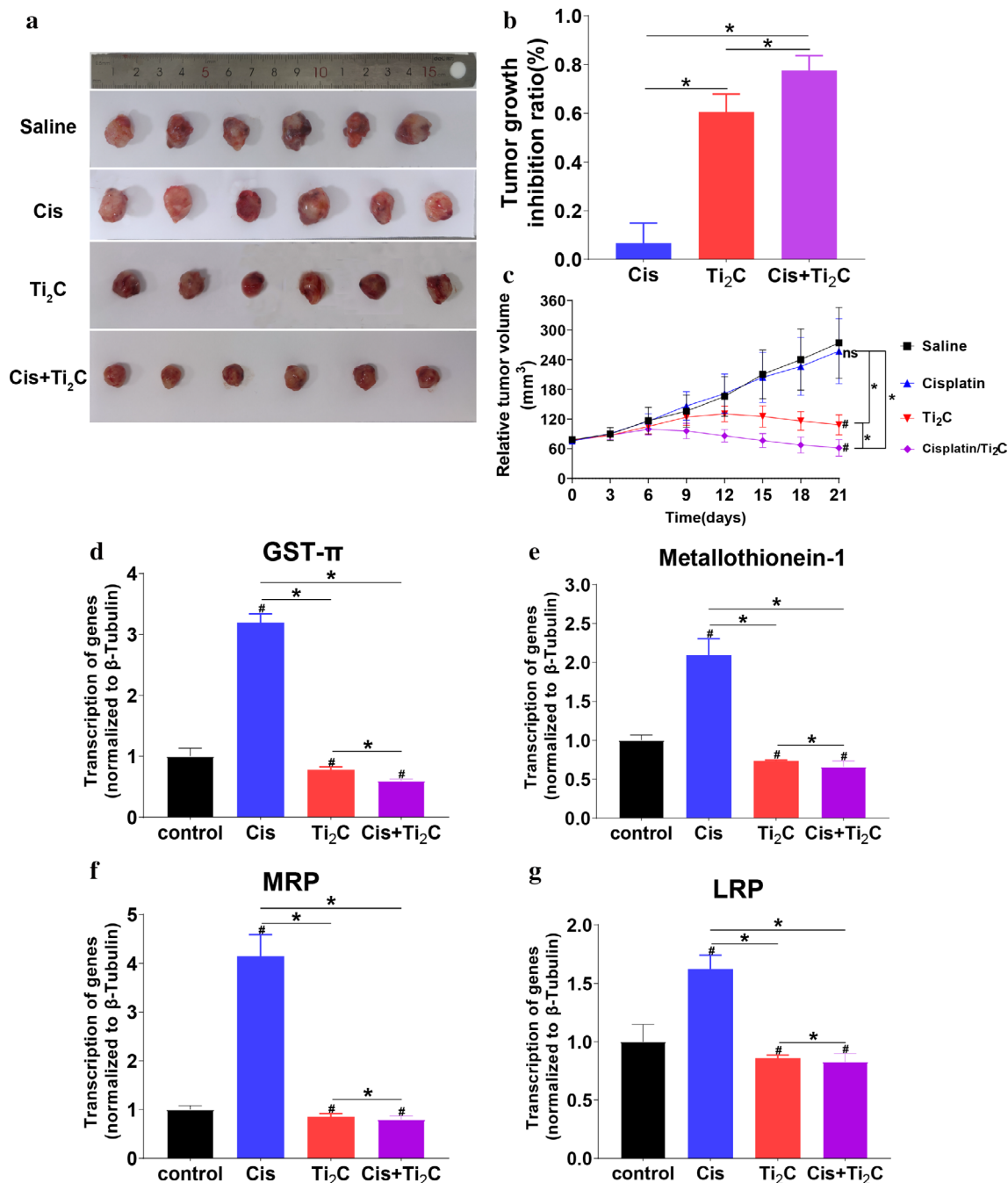

FIGURE 6 Treatment of A549/DDP xenograft tumors with saline, cisplatin, 2D Ti_2C, or cisplatin plus 2D Ti_2C. (a) Photographs of the solid tumors removed at the end of the study. (b) Percent tumor growth inhibition relative to tumor weight in the saline control. (c) Tumor volume measurements across the treatment period. mRNA expression of GST-π (d), metallothionein-1 (e), MRP (f), and LRP (g) in transplantation tumor model in vivo. *$p < 0.05$. # indicates a significant difference with the control group. ns indicates not significant with the control group
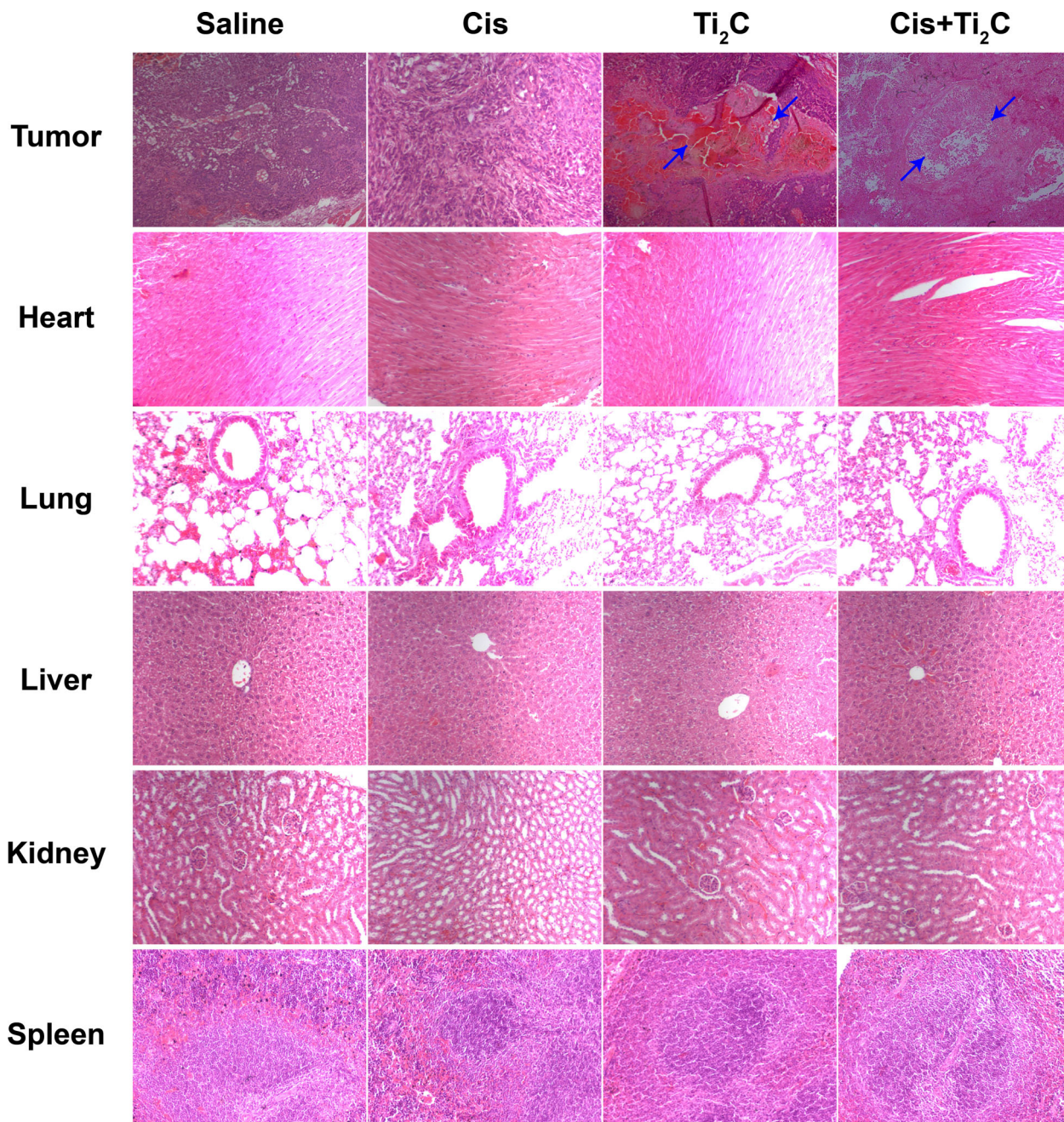
FIGURE 7 Histological assessments of tumor tissues (×10) and major organs (×20) after mice bearing A549/DDP xenografts were injected with saline, cisplatin, 2D Ti$_2$C, or cisplatin plus 2D Ti$_2$C. Blue arrows indicate necrotic areas

results indicate that 2D Ti$_2$C plays a decisive role in inhibiting two key antioxidant proteins. A possible reason for this is that the high surface area of 2D Ti$_2$C and its —O, —OH, and —F reactive groups provide a large number of electrons to bind to the electron-absorbing thiol residues, which are present in GSH, proteins such as metallothionein, and certain drugs. Interaction with thiol groups in metallothionein likely alters its structure or prevents it from interacting with other partners such as cisplatin, while a feedback loop might lead to a decrease in expression at the gene level. Taken together, our results illustrate how 2D Ti$_2$

C may overcome cisplatin resistance by depleting the antioxidant system in multiple aspects.

2D Ti$_2$C mediates the decrease in expression of key drug resistance genes

In drug-resistant NSCLC, some key genes such as MRP, LRP, and MDR-1, whose high expression is confirmed to be closely associated with drug resistance, are in turn regulated by changes in the upstream antioxidant reserve system,[65,66]

so we evaluated the expression of these genes after cisplatin and/or 2D Ti$_2$C treatment. MRP is an important member of the cellular transmembrane protein family, responsible for the internal and external exchange of cisplatin in cells.[67] In most cases, MRP confers drug resistance by excreting GSH-conjugated drug directly out of the cell or alters the drug's intracellular distribution.[68–70] Its expression can be positively regulated by GSH levels in cells, which could serve as another means of preventing intracellular cisplatin accumulation in resistant NSCLC.[71] We found that the MRP transcript level was elevated after stimulation with cisplatin in drug-resistant cells, suggesting an activation signal of MRP transcription to counteract cisplatin. In contrast, MRP transcription was downregulated by 2D Ti$_2$C with or without cisplatin (Figure 5(a)). This may be due to a decrease in the proportion of GSH, which normally would conjugate to cisplatin and would require MRP for transport, so a depletion of GSH likely constitutes a signal that MRP is not needed.[37,40] LRP is another protein that is overexpressed in tumor cells. It can be localized to the cytoplasm and the nucleus, particularly at nuclear pore complexes, and it can block cisplatin entry into the nucleus by blocking the nuclear pores and by sequestering cisplatin into exocytotic vesicles.[72] In our study, the expression of LRP was significantly reduced after 2D Ti$_2$C treatment and further reduced after the co-administration of cisplatin (Figure 5(b),(d)). Previous literature has reported that depletion of GSH reserves can lead to impaired cell membrane repair,[73] which in turn blocks the vesicle formation pathway involving LRP expression.[74] The MDR-1 gene is responsible for encoding P-glycoprotein, a cell membrane-bound adenosine triphosphate-binding cassette transporter protein that actively extrudes cisplatin from cancer cells, leading to drug resistance.[75] Similar to the pattern for LRP, we also found an increase in MDR-1 transcription after cisplatin treatment alone, while 2D Ti$_2$C with or without cisplatin led to a significant reduction of MDR-1 expression at both the transcript and protein levels (Figure 5(c),(d)). The decreased expression of each of these drug resistance genes correlated with the effective accumulation of cisplatin in cells (Table 2), thus contributing to increased sensitivity to cisplatin-induced cell death.

Reversal of drug resistance in NSCLC by 2D Ti$_2$C in vivo

In our in vitro experiments, we have demonstrated that 2D Ti$_2$C can re-sensitize A549/DDP cells to cisplatin by depleting intracellular GSH content and downregulating the expression of genes that are involved in GSH homeostasis, protection from free radicals, or multidrug resistance. To determine if these findings are relevant in vivo, we generated a subcutaneous xenograft model of A549/DDP tumors in Balb/c nude mice and tested tumor response to cisplatin and 2D Ti$_2$C. Our results revealed that cisplatin alone led to only 8.94% ± 6.62% reduction in tumor size compared with the

control group, confirming that the subcutaneous tumors still maintained some cisplatin-resistance in vivo. In contrast, the tumor volume was significantly reduced by 61.82% ± 14.35% relative to the saline control when 2D Ti$_2$C was injected, and when 2D Ti$_2$C and cisplatin were co-injected the tumor volume was reduced by 77.68% ± 5.27% (Figure 6(a)–(c)). To validate the reversal of resistance mechanisms in vivo, we also explored the gene expression of GST-π, metallothionein-1, MRP, and LRP (Figure 6(d)–(g)). The results showed that 2D Ti$_2$C also reduced the expression of the relevant genes in in vivo conditions, and co-administration of 2D Ti$_2$C with cisplatin maintained the decreased levels. Our results suggest that (1) 2D Ti$_2$C itself can directly inhibit chemoresistant tumor growth, (2) 2D Ti$_2$C can re-sensitize resistant tumors to cisplatin, and (3) mechanisms for reversing chemoresistance also apply in vivo.

In vivo biosafety of 2D Ti$_2$C

We performed histological assessment of tumor tissues and major organs to determine the toxicity of 2D Ti$_2$C and cisplatin in our in vivo tumor model. We found that 2D Ti$_2$C, neither alone nor in combination, caused any significant pathological changes in the major organs throughout the treatment, indicating that 2D Ti$_2$C and cisplatin were safe at the doses we used. In comparison, we observed some degree of liquefactive necrosis of the tumor tissues (blue arrows in Figure 7) from the Ti$_2$C and cisplatin-plus-Ti$_2$C treatment groups, and the extent of necrosis is more pronounced in the latter group. These observations suggest that 2D Ti$_2$C can selectively enhance cisplatin cytotoxicity in chemoresistant tumor tissues without being toxic to other nontumor tissues.

CONCLUSION

Our studies show the promise of reversing the drug resistance of NSCLC by nanomaterial 2D Ti$_2$C. 2D Ti$_2$C has advantageous physicochemical properties, including nanometer thickness, large specific surface area, and abundant —O, —OH, and —F reactive groups on the surface, making it more accessible to interact with a variety of intracellular proteins. Our in vitro experiments revealed that 2D Ti$_2$C can not only inhibit the proliferation and induce apoptosis of cisplatin-resistant A549/DDP cells by itself, but also re-sensitizes the NSCLC cells to cisplatin toxicity by depleting the intracellular antioxidant reserve system, while enhancing cisplatin uptake in NSCLC cells and downregulating the expression of key drug resistance genes. Our in vivo experiments also validated the effect and mechanism of 2D Ti$_2$C in reversing drug resistance in NSCLC and further demonstrated the safety of 2D Ti$_2$C in normal organs. Collectively, our results demonstrate that 2D Ti$_2$C is a highly promising novel agent for treating chemoresistant NSCLC.

CONFLICT OF INTEREST

The author reports no conflicts of interest in this work.

ORCID

Jiao Sun https://orcid.org/0000-0002-2300-0500

REFERENCES

1. NSCLC Meta Analyses Collaborative Group. Chemotherapy in addition to supportive care improves survival in advanced non-small-cell lung cancer: a systematic review and metaanalysis of individual patient data from 16 randomized controlled trials. J Clin Oncol. 2008; 26(28):4617.

2. Group NCLCC. Chemotherapy in non-small cell lung cancer: a meta-analysis using updated data on individual patients from 52 randomised clinical trials. BMJ. 1995;311(7010):899.

3. Wang J, Lee JS, Kim D, Zhu L. Exploration of zinc oxide nanoparticles as a multitarget and multifunctional anticancer nanomedicine. ACS Appl Mater Interfaces. 2017;9(46):39971–84.

4. Cai H, Wang X, Zhang H, Sun L, Pan D, Gong Q, et al. Enzyme-sensitive biodegradable and multifunctional polymeric conjugate as theranostic nanomedicine. Appl Mater Today. 2018;11:207.

5. Zhuang Y, Li L, Feng L, Wang S, Su H, Liu H, et al. Mitochondrion-targeted selenium nanoparticles enhance reactive oxygen species-mediated cell death. Nanoscale. 2020;12(3):1389–96.

6. Swanner J, Fahrenholtz CD, Tenvooren I, Bernish BW, Sears JJ, Hooker A, et al. Silver nanoparticles selectively treat triple-negative breast cancer cells without affecting non-malignant breast epithelial cells in vitro and in vivo. FASEB Bioadv. 2019; 1(10):639–60.

7. Li K, Chen B, Xu L, Feng J, Xia G, Cheng J, et al. Reversal of multidrug resistance by cisplatin-loaded magnetic Fe3O4 nanoparticles in A549/DDP lung cancer cells in vitro and in vivo. Int J Nanomedicine. 2013;8:1867–77.

8. Gokduman K. Sensitization of cisplatin-resistant ovarian cancer cells by magnetite iron oxide nanoparticles: an in vitro study. Nanomedicine (Lond). 2019;14(24):3177–91.

9. Bejjanki NK, Xu H, Xie M. GSH triggered intracellular aggregated-cisplatin-loaded iron oxide nanoparticles for overcoming cisplatin resistance in nasopharyngeal carcinoma. J Biomater Appl. 2021;36(1):45–54.

10. Mei L, Zhu S, Yin W, Chen C, Nie G, Gu Z, et al. Two-dimensional nanomaterials beyond graphene for antibacterial applications: current progress and future perspectives. Theranostics. 2020;10(2):757–81.

11. Silva MM, Rocha CRR, Kinker GS, Pelegrini AL, Menck CFM. The balance between NRF2/GSH antioxidant mediated pathway and DNA repair modulates cisplatin resistance in lung cancer cells. Sci Rep. 2019;9(1):1.

12. Parker LJ, Ciccone S, Italiano LC, Primavera A, Oakley AJ, Morton CJ, et al. The anti-cancer drug chlorambucil as a substrate for the human polymorphic enzyme glutathione transferase P1-1: kinetic properties and crystallographic characterisation of allelic variants. J Mol Biol. 2008;380(1):131–44.

13. Yuan Y, Xu S, Zhang CJ, Zhang R, Liu B. Dual-targeted activatable photosensitizers with aggregation-induced emission (AIE) characteristics for image-guided photodynamic cancer cell ablation. J Mater Chem B. 2016;4(1):169–76.

14. Zhang K, Mack P, Wong KP. Glutathione-related mechanisms in cellular resistance to anticancer drugs. Int J Oncol. 1998;12(4): 871–82.

15. Couto N, Wood J, Barber J. The role of glutathione reductase and related enzymes on cellular redox homoeostasis network. Free Radic Biol Med. 2016;95:27–42.

16. Dalton TP, Shertzer HG, Puga A. Regulation of gene expression by reactive oxygen. Annu Rev Pharmacol Toxicol. 1999;39:67–101.

17. Chen Y, Wu Y, Sun B, Liu S, Liu H. Two-dimensional nanomaterials for cancer nanotheranostics. Small. 2017;13(10):1603446.

18. Rozmysowska-Wojciechowska A, Wojciechowski T, Ziemkowska W, Chlubny L, Jastrzbska AM. Surface interactions between 2D Ti3C2/Ti2C MXenes and lysozyme. Appl Surf Sci. 2018;473:409.

19. Jastrzebska AM, Szuplewska A, Wojciechowski T, Chudy M, Ziemkowska W, Chlubny L, et al. In vitro studies on cytotoxicity of delaminated Ti3C2 MXene. J Hazard Mater. 2017;339(Oct 5): 1–8.

20. Zhong WZ, Wang Q, Mao WM, Xu ST, Wu L, Shen Y, et al. Gefitinib versus vinorelbine plus cisplatin as adjuvant treatment for stage II-IIIA (N1-N2) EGFR-mutant NSCLC (ADJUVANT/CTONG1104): a randomised, open-label, phase 3 study. Lancet Oncol. 2018;19(1): 139–48.

21. Rizvi NA, Hellmann MD, Brahmer JR, Juergens RA, Borghaei H, Gettinger S, et al. Nivolumab in combination with platinum-based doublet chemotherapy for first-line treatment of advanced non-small-cell lung cancer. J Clin Oncol. 2016;34(25):2969–79.

22. Liu F, Zhou A, Chen J, Jia J, Zhou W, Wang L, et al. Preparation of Ti3C2 and Ti2C MXenes by fluoride salts etching and methane adsorptive properties. Appl Surf Sci. 2017;416:781.

23. Xiong X, Arvizo RR, Saha S, Robertson DJ, McMeekin S, Bhattacharya R, et al. Sensitization of ovarian cancer cells to cisplatin by gold nanoparticles. Oncotarget. 2014;5(15):6453–5.

24. Chang PY, Peng SF, Lee CY, Lu CC, Tsai SC, Shieh TM, et al. Curcumin-loaded nanoparticles induce apoptotic cell death through regulation of the function of MDR1 and reactive oxygen species in cisplatin-resistant CAR human oral cancer cells. Int J Oncol. 2013; 43(4):1141–50.

25. Ivask A, Juganson K, Bondarenko O, Mortimer M, Aruoja V, Kasemets K, et al. Mechanisms of toxic action of Ag, ZnO and CuO nanoparticles to selected ecotoxicological test organisms and mammalian cells in vitro: a comparative review. Nanotoxicology. 2014;8(Suppl 1):57–71.

26. Liu J, Li Q, Zhang J, Huang L, Qi C, Xu L, et al. Safe and effective reversal of cancer multidrug resistance using sericin-coated mesoporous silica nanoparticles for lysosome-targeting delivery in mice. Small. 2017;13(9):1602567.

27. Tammam SN. Lipid based nanoparticles as inherent reversing agents of multidrug resistance in cancer. Curr Pharm Des. 2017;23(43):6714.

28. JastrzęBska A. Biological activity and bio-sorption properties of the Ti2C studied by means of zeta potential and SEM. Int J Electrochem Sci. 2016;12:2159–72.

29. Zucker I, Werber JR, Fishman ZS, Hashmi SM, Gabinet UR, Lu X, et al. Loss of phospholipid membrane integrity induced by two-dimensional nanomaterials. Environ Sci Technol Lett. 2017;4(10):404.

30. Dąbruś D, Kiełbasiński R, Grabarek BO, Boroń D. Evaluation of the impact of cisplatin on variances in the expression pattern of leptin-related genes in endometrial cancer cells. Int J Mol Sci. 2020;21(11): 4135.

31. Singh M, Chaudhry P, Fabi F, Asselin E. Cisplatin-induced caspase activation mediates PTEN cleavage in ovarian cancer cells: a potential mechanism of chemoresistance. BMC Cancer. 2013;13(1):1.

32. Park BH, Lim JE, Jeon HG, Seo SI, Lee HM, Choi HY, et al. Curcumin potentiates antitumor activity of cisplatin in bladder cancer cell lines via ROS-mediated activation of ERK1/2. Oncotarget. 2016;7(39): 63870.

33. Chen P, Yan LT. Physical principles of graphene cellular interactions: computational and theoretical accounts. J Mater Chem B. 2017;5(23): 4290–306.

34. Duan G, Zhang Y, Luan B, Weber JK, Zhou RW, Yang Z, et al. Graphene-induced pore formation on cell membranes. Sci Rep. 2017; 7:42767.

35. Kuo MT, Chen HH, Song IS, Savaraj N, Ishikawa T. The roles of copper transporters in cisplatin resistance. Cancer Metastasis Rev. 2007; 26(1):71–83.

36. Lan D, Wang L, He R, Ma J, Bin Y, Chi X, et al. Exogenous glutathione contributes to cisplatin resistance in lung cancer A549 cells. Am J Transl Res. 2018;10(5):1295–309.

37. Leslie EM, Ito K, Upadhyaya P, Hecht SS, Deeley RG, Cole SPC. Transport of the β-O-glucuronide conjugate of the tobacco-specific carcinogen 4-(methylnitrosamino)-1-(3-pyridyl)-1-butanol (NNAL) by the multidrug resistance protein 1 (MRP1): requirement for glutathione or a non-sulfur-containing analog. J Biol Chem. 2001;276(30): 27846.

38. Zhang S, Zhong X, Yuan H, Guo Y, Song D, Qi F, et al. Interfering in apoptosis and DNA repair of cancer cells to conquer cisplatin resistance by platinum (IV) prodrugs. Chem Sci. 2020;11(15):3829.

39. Paulusma CC, Geer MAV, Evers R, Heijn M, Ottenhoff R, Borst P, et al. Canalicular multispecific organic anion transporter/multidrug resistance protein 2 mediates low-affinity transport of reduced glutathione. Biochem J. 1999;338(2):393.

40. Chen HHW, Kuo MT. Role of glutathione in the regulation of Cisplatin resistance in cancer chemotherapy. Met Based Drugs. 2010; 2010:430939.

41. Brozovic A, Ambriović-Ristov A, Osmak M. The relationship between cisplatin-induced reactive oxygen species, glutathione, and BCL-2 and resistance to cisplatin. Crit Rev Toxicol. 2010;40(4):347–59.

42. Chakravarthi S, Jessop CE, Bulleid NJ. The role of glutathione in disulphide bond formation and endoplasmic-reticulum-generated oxidative stress. EMBO Rep. 2006;7(3):271–5.

43. Blair SL, Heerdt P, Sachar S, Abolhoda A, Burt M. Glutathione metabolism in patients with non-small cell lung cancers. Cancer Res. 1997; 57(1):152–5.

44. Lin L, Chen C, Ho C, Liu J, Liu T, Chern C. γ-glutamylcysteine synthetase (γ-GCS) as a target for overcoming chemo-and radio-resistance of human hepatocellular carcinoma cells. Life Sci. 2018; 198:25.

45. Traverso N, Ricciarelli R, Nitti M, Marengo B, Furfaro AL, Pronzato MA, et al. Role of glutathione in cancer progression and chemoresistance. Oxid Med Cell Longev. 2013;2013:972913.

46. Kohsaka S, Takahashi K, Wang L, Tanino M, Kimura T, Nishihara H, et al. Inhibition of GSH synthesis potentiates temozolomide-induced bystander effect in glioblastoma. Cancer Lett. 2013;331(1):68.

47. Das GC, Bacsi A, Shrivastav M, Hazra TK, Boldogh I. Enhanced γ-glutamylcysteine synthetase activity decreases drug-induced oxidative stress levels and cytotoxicity. Mol Carcinog. 2006; 45(9):635.

48. Zeng X, Ye Z, Yang W. Relation between the expressions of oncogene c-jun, c-fos and the expressions of γ-glutamylcysteine synthetase (γ-GCS) and glutathion (GSH) in drug-resistant human bladder cancer line. Cancer Res Prev Treat. 2004;31(1):30–2.

49. Ng CF, Schafer FQ, Buettner GR, Rodgers V. The rate of cellular hydrogen peroxide removal shows dependency on GSH: mathematical insight into in vivo H2O2 and GPx concentrations. Free Radic Res. 2007;41(11):1201.

50. Viswanathan VS, Ryan MJ, Dhruv HD, Gill S, Eichhoff OM, Seashore-Ludlow B, et al. Dependency of a therapy-resistant state of cancer cells on a lipid peroxidase pathway. Nature. 2017; 547(7664):453.

51. Liu K, Jin M, Xiao L, Liu H, Wei S. Distinct prognostic values of mRNA expression of glutathione peroxidases in non-small cell lung cancer. Cancer Manag Res. 2018;10:2997.

52. Geng M, Wang L, Chen X, Cao R, Li P. The association between chemosensitivity and Pgp, GST-π and Topo II expression in gastric cancer. Diagn Pathol. 2013;8(1):1.

53. Kulaksiz-Erkmen G, Dalmizrak O, Dincsoy-Tuna G, Dogan A, Ogus IH, Ozer N. Amitriptyline may have a supportive role in cancer treatment by inhibiting glutathione S-transferase pi (GST-π) and alpha (GST-α). J Enzyme Inhib Med Chem. 2013;28(1):131.

54. Tang Y, Xuan X, Li M, Dong Z. Roles of GST-π and polβ genes in chemoresistance of esophageal carcinoma cells. Asian Pac J Cancer Prev. 2013;14(12):7375.

55. Townsend DM, Manevich Y, He L, Hutchens S, Pazoles CJ, Tew KD. Novel role for glutathione S-transferase pi. Regulator of protein S-glutathionylation following oxidative and nitrosative stress. J Biol Chem. 2009;284(1):436–45.

56. Yang L, Du C, Wu L, Yu J, An X, Yu W, et al. Cytokine-induced killer cells modulates resistance to cisplatin in the A549/DDP cell line. J Cancer. 2017;8(16):3287.

57. Lin C, Xie L, Lu Y, Hu Z, Chang J. miR-133b reverses cisplatin resistance by targeting GSTP1 in cisplatin-resistant lung cancer cells. Int J Mol Med. 2018;41(4):2050.

58. Gajra A, Vajpayee N, Wade M, Gamble GP, Rajan A, Graziano SL. Expression of the glutathione-S-transferase π (GST-π) protein correlates with survival in patients with stage I non-small cell lung cancer (NSCLC). J Clin Oncol. 2007;25(18_suppl):21065.

59. Wang M, Xu Y, Pan S, Zhang J, Zhong A, Song H, et al. Long-term heavy metal pollution and mortality in a Chinese population: an ecologic study. Biol Trace Elem Res. 2011;142(3):362–79.

60. Duan Q, Wang T, Zhang N, Perera V, Liang X, Abeysekera IR, et al. Propylthiouracil, perchlorate, and thyroid-stimulating hormone modulate high concentrations of iodide instigated mitochondrial superoxide production in the thyroids of metallothionein I/II knockout mice. Endocrinol Metab (Seoul). 2016;31(1):174–84.

61. Ruttkay-Nedecky B, Nejdl L, Gumulec J, Zitka O, Masarik M, Eckschlager T, et al. The role of metallothionein in oxidative stress. Int J Mol Sci. 2013;14:6044–66.

62. Si M, Lang J. The roles of metallothioneins in carcinogenesis. J Hematol Oncol. 2018;11(1):107.

63. Borchert S, Suckrau PM, Walter RFH, Wessolly M, Mairinger FD. Impact of metallothionein-knockdown on cisplatin resistance in malignant pleural mesothelioma. Sci Rep. 2020;10(1):18677.

64. Matsumoto Y, Oka M, Sakamoto A, Narasaki F, Kohno S. Enhanced expression of metallothionein in human non-small-cell lung carcinomas following chemotherapy. Anticancer Res. 1997; 17(5B):3777.

65. Jin WS, Kong ZL, Shen ZF, Jin YZ, Chen GF. Regulation of hypoxia inducible factor-1α expression by the alteration of redox status in HepG2 cells. J Exp Clin Cancer Res. 2011;30(1):61.

66. Tani M, Goto S, Kamada K, Mori K, Urata Y, Ihara Y, et al. Hammerhead ribozyme against gamma-glutamylcysteine synthetase attenuates resistance to ionizing radiation and cisplatin in human T98G glioblastoma cells. Cancer Sci. 2010;93(6):716–22.

67. Barrand MA, Heppell-Parton AC, Wright KA, Rabbitts PH, Twentyman PR. A 190-kilodalton protein overexpressed in non-P-glycoprotein-containing multidrug-resistant cells and its relationship to the MRP gene. J Natl Cancer Inst. 1994;86(2):110.

68. Longley DB, Johnston PG. Molecular mechanisms of drug resistance. J Pathol. 2005;205(2):275.

69. Burger H, Foekens JA, Look MP, Meijer-van Gelder ME, Klijn JG, Wiemer EA, et al. RNA expression of breast cancer resistance protein, lung resistance-related protein, multidrug resistance-associated proteins 1 and 2, and multidrug resistance gene 1 in breast cancer: correlation with chemotherapeutic response. Clin Cancer Res. 2003; 9(2):827.

70. Steinbach D, Wittig S, Cario G, Viehmann S, Mueller A, Gruhn B, et al. The multidrug resistance-associated protein 3 (MRP3) is associated with a poor outcome in childhood ALL and may account for the worse prognosis in male patients and T-cell immunophenotype. Blood. 2003;102(13):4493.

71. Suzuki T, Nishio K, Tanabe S. The MRP family and anticancer drug metabolism. Curr Drug Metab. 2001;2(4):367–77.

72. Mossink MH, Zon AV, Scheper RJ, Sonneveld P, Wiemer EA. Vaults: a ribonucleoprotein particle involved in drug resistance. Oncogene. 2003;22(47):7458–67.

73. Poellmann MJ, Lee RC. Repair and regeneration of the wounded cell membrane. Regen Eng Transl Med. 2017;3(3):111.

74. Izquierdo MA, Scheffer GL, Flens MJ, Shoemaker RH, Rome LH, Scheper RJ. Relationship of LRP-human major vault protein to in vitro and clinical resistance to anticancer drugs. Cytotechnology. 1996;19(3):191.

75. Hour T, Chen J, Huang C, Guan JY, Lu SH, Hsieh CY, et al. Characterization of chemoresistance mechanisms in a series of cisplatin-resistant transitional carcinoma cell lines. Anticancer Res. 2000; 20(5A):3221.